Journal of Medicinal Chemistry

Article

pubs.acs.org/jmc

Pyrrolo[3,2-*b*]quinoxaline Derivatives as Types $I_{1/2}$ and II Eph Tyrosine Kinase Inhibitors: Structure-Based Design, Synthesis, and *in Vivo* Validation

Andrea Unzue,[†,§] Jing Dong,[‡,§] Karine Lafleur,[†] Hongtao Zhao,[‡] Emilie Frugier,[‡] Amedeo Caflisch,*[,‡] and Cristina Nevado*[,†]

[†]Department of Chemistry and [‡]Department of Biochemistry, University of Zürich, Winterthurerstrasse 190, CH-8057 Zürich, Switzerland

Supporting Information

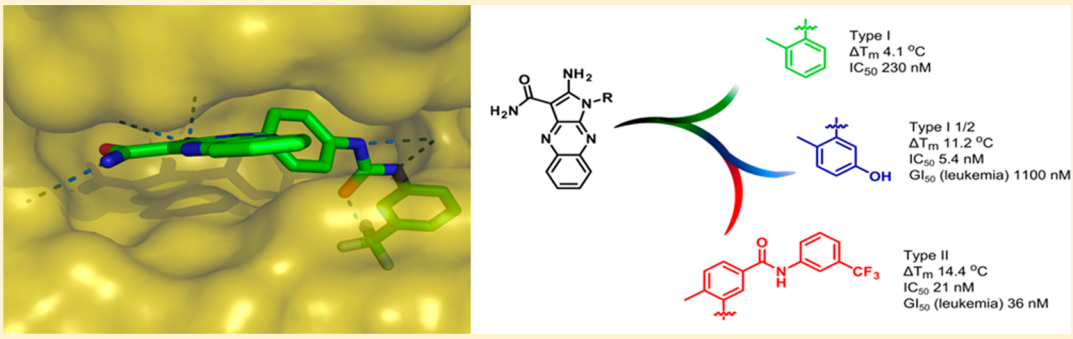

ABSTRACT: The X-ray crystal structures of the catalytic domain of the EphA3 tyrosine kinase in complex with two type I inhibitors previously discovered *in silico* (compounds **A** and **B**) were used to design type $I_{1/2}$ and II inhibitors. Chemical synthesis of about 25 derivatives culminated in the discovery of compounds **11d** (type $I_{1/2}$), **7b**, and **7g** (both of type II), which have low-nanomolar affinity for Eph kinases *in vitro* and a good selectivity profile on a panel of 453 human kinases (395 nonmutant). Surface plasmon resonance measurements show a very slow unbinding rate (1/115 min) for inhibitor **7m**. Slow dissociation is consistent with a type II binding mode in which the hydrophobic moiety (trifluoromethyl-benzene) of the inhibitor is deeply buried in a cavity originating from the displacement of the Phe side chain of the so-called DFG motif as observed in the crystal structure of compound **7m**. The inhibitor **11d** displayed good *in vivo* efficacy in a human breast cancer xenograft.

I. INTRODUCTION

Several protein kinases are relevant targets for the treatment of diseases ranging from cancer, inflammation, and cardiovascular conditions to immune related disorders.[1,2] Over the past decade, more than 13 small-molecule kinase inhibitors have been approved by the FDA as therapeutics for various human pathologies.[3−6] In this context, receptor tyrosine kinases play a prominent role, as they are involved in a number of biologically relevant processes for cancer development including oncogenic regulation, cell signal transduction, proliferation, and survival among many others.[7,8] Although irreversible inhibitors that form covalent bonds with cysteine or other nucleophilic residues in the ATP-binding pocket have been recently explored,[9,10] ATP competitive, noncovalent inhibitors are much more abundant and, depending on the binding mode with their protein target, are classified as type I−IV.[11] Most kinase inhibitor drugs are of type I, i.e., they are direct competitors of ATP within the catalytic site of the phosphorylated active conformation of the protein.[12] However, because of the strong similarities between the ATP binding pocket of all human kinases, alternative approaches providing selective binders have been sought.[13−18] Small molecules forming additional interactions with hydrophobic regions adjacent to the ATP binding site are termed type $I_{1/2}$ inhibitors. Alternatively, type II inhibitors target the kinase catalytic site but bind to the inactive conformation of the protein, thus exploring a pocket generated upon displacement of the phenylalanine side chains of the DFG motif.[4] Type III inhibitors, also known as allosteric inhibitors, target areas of the kinase not related to the catalytic domain, whereas type IV do so without competing with ATP. Higher degrees of selectivity are to be expected with the latter two inhibitor types.[19]

Recently, our groups have focused on the *in silico* design, synthesis, and computational-aided optimization of potent and selective receptor tyrosine kinase inhibitors. Successful campaigns have yielded single-digit nanomolar EphB4 inhibitors whose potential antiproliferative activities have been characterized by cellular assays.[20−22] Furthermore, the predicted binding mode could also be confirmed by X-ray diffraction analysis of their complexes with EphA3. Given the

Received: June 18, 2014
Published: July 30, 2014

critical role of Eph receptors and (Eph)−ephrin signaling in tumor growth and progression,[23] a subset of these compounds are currently being pursued toward preclinical development.

Here we describe a multidisciplinary campaign toward the design of novel and potent, type $I_{1/2}$ and II tyrosine kinase inhibitors based on the crystal structure of two type I inhibitors. The parent pyrrolo[3,2-*b*]quinoxaline scaffold was decorated with characteristic functional groups present in previously successful type II binders, thus speeding up the hit to lead optimization campaign. The binding kinetics of the low-nanomolar derivatives **11d** (type I1/2) and **7m** (type II) were characterized by surface plasmon resonance (SPR) measurements. Extensive profiling by biochemical (competition binding) and cellular assays, together with pharmacokinetic measurements in mice resulted in the prioritization of inhibitor **11d** for final validation *in vivo* by a human breast cancer xenograft.

II. CRYSTAL STRUCTURES OF TYPE I INHIBITORS A AND B WITH EPHA3

II.1. Docking Validation by X-ray Diffraction Analysis of Binding Complex. Recently, we reported the discovery of two type I EphB4 inhibitors **A** and **B** by automated docking.[24] The *in silico* predicted binding mode of these molecules is confirmed here by X-ray diffraction analysis of the catalytic domain of EphA3 in complex with both **A** and **B** (Figure 1).

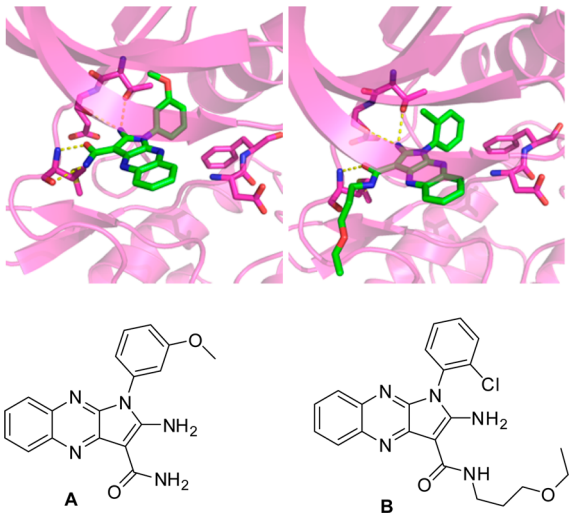

Figure 1. Crystal structures of the catalytic domain of the tyrosine kinase EphA3 in complex with the high-nanomolar inhibitors **A** (left, pdb code 4P4C) and **B** (right, pdb code 4P5Q). The ATP binding site of the EphA3 kinase is shown in magenta ribbons, while the side chains mentioned in the text and the inhibitors are shown by sticks (with carbon atoms in magenta and green, respectively).

The pyrrolo[3,2-*b*]quinoxaline scaffold occupies the ATP binding site with the phenyl substituent nestled into the so-called hydrophobic pocket. The amino substituent at position 2 of the pyrrole ring is involved in a bifurcated hydrogen bond with the side chain hydroxyl of the Thr693 gatekeeper and the backbone carbonyl of Glu694. Furthermore, in the structure with inhibitor **A**, the amide substituent at position 3 of the pyrrole ring is optimally oriented for two hydrogen bonds with the backbone polar groups of Met696 so that **A** forms a total of three hydrogen bonds with the backbone of the hinge region. Only two hydrogen bonds with the same region are observed for inhibitor **B** due to the ethoxy-propyl substitution at the nitrogen of the amide whose trans configuration prevents it from acting as donor to the carbonyl group of Met696. The lack of this hydrogen bond is consistent with the about 10-fold weaker affinity of inhibitor **B** with respect to **A** (IC_{50} of 300 nM for EphB4),[24] which might also originate, at least in part, from the different substituents of the phenyl ring in the hydrophobic pocket, i.e., $-OCH_3$ and −Cl in **A** and **B**, respectively.

II.2. Design of Type $I_{1/2}$ and Type II Derivatives Based on the X-ray Crystal Structure of the Type I Inhibitors A and B. On the basis of our previous experience[20,22] and earlier reports toward the synthesis of potent type I kinase inhibitors,[25] several modifications within the phenyl ring were designed in order to fine-tune the interactions of the quinoxaline inhibitors with the threonine gatekeeper residue (Thr693) of EphB4. Because of the rather limited space around the phenyl group revealed by the binding modes of **A** and **B**, the introduction of small substituents was envisioned, including the incorporation of a methyl and a hydroxyl group at positions 2 and 5, a combination that had been successfully exploited in our previous studies developing nanomolar inhibitors of EphB4.[20]

In addition, the binding modes of inhibitors **A** and **B** suggested the possibility to extend the quinoxaline scaffold into the allosteric binding site by substitution of the phenyl ring, resulting in type II inhibitors. Our design campaign targeting the back pocket of the kinase relied on the introduction of a variety of substituents, some of which are present in type II inhibitors. The so-called "tail" moiety of type II inhibitors, located within the allosteric binding site, is characterized by a hydrogen bond donor−acceptor pair (usually an amide or an urea), linked to a hydrophobic substituent that occupies the newly formed pocket in the DFG-out conformation of the kinase.[4,7,12] Amide, urea, and thiourea linkers were incorporated onto the quinoxaline scaffold and attached to a *m*-CF_3-phenyl moiety present in some type II kinase inhibitors, in analogy to AAL993,[26] sorafenib,[27,28] and GNF-5837[29] (**7b−d**, **7g−i**, **7l**, **7m**, and **12n**). A cyclopropyl ring, a common motif in p38α isoform selective kinase inhibitors,[30−32] was also introduced (**7a**, **7f**, and **7k**). In an effort to increase the hydrophobic interactions within the allosteric binding site, a 4-methyl imidazole ring was added aiming to mimic the well-known drug nilotinib[33] (**7e** and **7j**). In order to increase the solubility, methyl or fluoro substituents were placed in ortho-relative position (**7c−e** and **7h−j**), therefore distorting the planarity of the molecules.[34] The results in Table 1 underline that, although the identification of substituents successfully binding the allosteric pocket based on known inhibitors was not *a priori* obvious, this was nonetheless an efficient strategy to obtain potent and selective type II kinase inhibitors in a time- and cost-effective manner.

III. CHARACTERIZATION OF NEW TYPE $I_{1/2}$ AND II INHIBITORS

III.1. Synthesis. The synthesis of 1*H*-pyrrolo[2,3-*b*]-quinoxaline derivatives **6** and **7** is shown in Scheme 1. Compound **1** was prepared according to previously reported procedures by condensation of commercially available 2,3-dichloroquinoxaline with malononitrile in the presence of sodium hydride.[35,36] The substitution of the chlorine at position 3 with commercially available anilines **2a−i** followed by cyclization afforded intermediates **4a−i**.[37] The reaction with synthetically prepared anilines **3a−n** delivered tricyclic intermediates **5a−n** (Scheme 1).

Table 1. EphA3/EphB4 Inhibition Data for the Synthesized Quinoxaline Derivatives

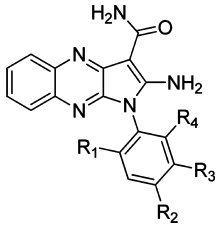

Compound	Type of binding	R_1	R_2	R_3	R_4	Thermal shift (degrees)[a]	FRET[b] enzymatic assay (% of inhibition at 1 μM)	Cellular IC_{50} (nM)[c]
6a	I	Me	H	H	H	4.1	66	230
6b	I	Me	H	H	Me	2.6	36	4400
6c	I	Me	H	H	Cl	2.6	45	2800
6d	I	Me	H	OMe	H	1.5	23	720
6e	$I_{1/2}$	Me	H	CH_2OH	H	3.6	68	160
6f	I	Cl	H	H	H	3.0	90	-
6g	I	F	H	H	H	2.7	30	-
6h	$I_{1/2}$	H	H	OH	H	7.2	98	-
6i	$I_{1/2}$	H	H		H	0.1	7	-
11d	$I_{1/2}$	Me	H	OH	H	11.2	105	5.4
7a	II	H	H		H	0.3	-	-
7b	II	H	H		H	7.6	-	20
7c	II	Me	H		H	12.3	-	14
7d	II	F	H		H	10.9	-	15
7e	II	Me	H	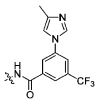	H	15.8	-	170
7f	II	H	H		H	0.6	-	-
7g	II	H	H		H	9.1	-	20
7h	II	Me	H		H	14.4	-	21
7i	II	F	H		H	13.0	-	24
7j	II	Me	H		H	16.2	-	270
7k	II	H	H		H	0.3	-	-
7l	II	H	H	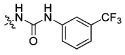	H	0.7	-	-
7m	II	H	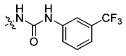	H	H	14.3	-	89
12n	II	H	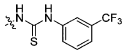	H	H	9.9	-	560

[a]Average values of triplicate measurements. The standard deviation is smaller than 0.5 degrees. [b]FRET-based enzymatic assay was carried out using the Z-LYTE Kinase Assay Kit−Tyr 1 Peptide (Invitrogen) following the vendor instructions. [c]Cell IC_{50} values were measured in a cellular phosphorylation assay using MEF cells overexpressing EphB4 at Proqinase.

The preparation of the noncommercially available anilines **3a−m** used in the above-mentioned condensation reaction has been summarized in Scheme 2. Anilines **3a−e**, bearing a N-amide group in meta-relative position, were obtained by

Scheme 1[a]

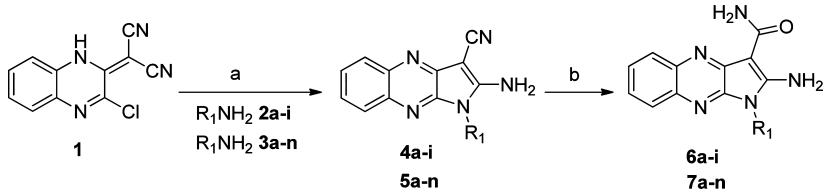

[a]Reagents and reaction conditions. (a) Protocol I: R_1NH_2 **2a–i**, **3a–d**, **3f–i**, **3k–l**, **3n** (1–4 equiv), EtOH/toluene, 1:1, 130–160 °C, 4–12 h, 30–79%. Protocol II: R_1NH_2 **3e**, **3j**, **3m** (1–1.2 equiv), DMF, 80 °C, 12 h, 21–61%. (b) H_2SO_4, 25 °C, 30 min, 7–99%.

Scheme 2[a]

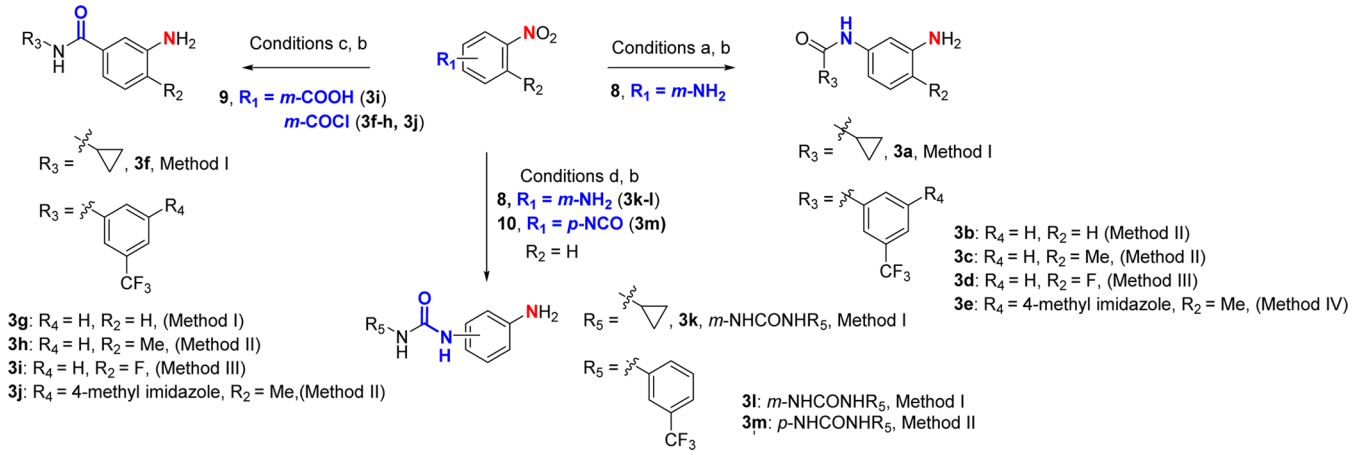

[a]Reagents and reaction conditions. Conditions (a) Method I: cyclopropanecarboxylic acid, TBTU, DIPEA, DMF, 25 °C, 15 h, 38%. Method II: 3-(trifluoromethyl)benzoyl chloride, Et_3N, DCM, 25 °C, 15 h, 54–99%. Method III: 3-(trifluoromethyl)benzoyl chloride, DIPEA, THF, 25 °C, 12 h, 48%. Method IV: benzoic acid, HOBt, EDC, DMF, 25 °C, 12 h, 64%. Conditions (b) for **3a**, **3b**, **3f**, **3g**, **3k** and **3l**, $SnCl_2.H_2O$, EtOH, 100 °C, 2 h, 53–92%; for **3c–e**, **3h–j**, and **3m**, 10% Pd/C (10 wt %), H_2, MeOH, 25 °C, 4–12 h, 44–99%. Conditions (c) Method I: amine, Et_3N, DCM, 25 °C, 15 h, 50–79%. Method II: aniline, DIPEA, THF, 25 °C, 12 h, 57–78%. Method III: (i) SO_2Cl, DCM, reflux, 3 h; (ii) 3-(trifluoromethyl)aniline, DCM, 25 °C, 12 h, 77%. Conditions (d) Method I: aniline, Et_3N, DCM, 25 °C, 1–3 d, 80–92%. Method II: 3-(trifluoromethyl)aniline, Et_3N, THF, 25 °C, 12 h, 60%.

condensation of 3-nitro-substituted anilines **8** with the corresponding readily available benzoyl chlorides (R_3COCl) or benzoic acids (R_3COOH)[38] using different protocols (Conditions a, Methods I–IV). Reduction of the nitro group with either $SnCl_2$ or Pd/C and H_2 (Conditions b, Supporting Information S12) furnished the desired intermediates. Anilines **3f–j** were prepared by condensation of the 3-nitro-substituted benzoic acid or benzoyl chlorides **9** with the corresponding anilines[39] under reaction conditions c. Reduction of the nitro group with $SnCl_2$ or Pd/C and H_2 delivered the corresponding anilines in 30–77% overall yields. Finally, anilines **3k–m**, bearing urea moieties at meta- and para-relative positions, were prepared by condensation of aniline **8** with the corresponding isocyanate (for **3k–l**) or by condensation of the isocyanate **10** with the respective commercially available aniline under reaction conditions d. Reduction of the nitro group under the conditions described above furnished the corresponding aniline-containing ureas **3k**, **3l**, and **3m** in 42, 85, and 41% yields, respectively. Aniline **3n** was prepared according to a previously reported procedure.[40]

Hydrolysis of the cyano group under strong acidic conditions furnished the desired type I and $I_{1/2}$ inhibitors **6a–i** and type II inhibitors **7a–n**, respectively. The presence of a cyano group in compounds **4** and **5** was confirmed by the presence of a characteristic IR band at around 2200 cm^{-1} and a ^{13}C NMR signal at 115–116 ppm, whereas the amino group appeared as a broad signal at 8 to 8.5 ppm in ^1H NMR.[37]

Two more inhibitors were prepared, first by demethylation of **6d** in the presence of BBr_3 under reflux to give the corresponding phenol derivative **11d**, and a second one by condensation of the aniline **7n** with *m*-CF_3-phenyl isothiocyanate, to give the corresponding thiourea **12n** (Scheme 3).

III.2. Biophysical Characterization. The thermodynamics and kinetics of binding of the designed quinoxaline inhibitors were investigated by an array of biophysical techniques including differential scanning fluorimetry, fluorescence resonance energy transfer (FRET) based enzymatic assays, and surface plasmon resonance (SPR). Differential scanning fluorimetry is a high throughput technique in which the increase in thermal stability of a folded protein upon ligand binding is detected by a fluorescent dye while measuring its melting temperature during denaturation.[41]

In order to allow the binding of type II inhibitors to the inactive form of the kinase, the protein (EphA3) was incubated in the presence of the compounds for 1 h. The results (shown in Table 1) highlight the differences in binding between type I, $I_{1/2}$, and II compounds, with type I being the weakest binders (1.5–4.1 °C) and type II the most potent (with up to 16 °C thermal shifts).

For type I inhibitors, the largest thermal shifts (ca. 4 °C) were obtained for *ortho*-methyl (**6a**) and *ortho*-chlorine (**6f**)

Scheme 3[a]

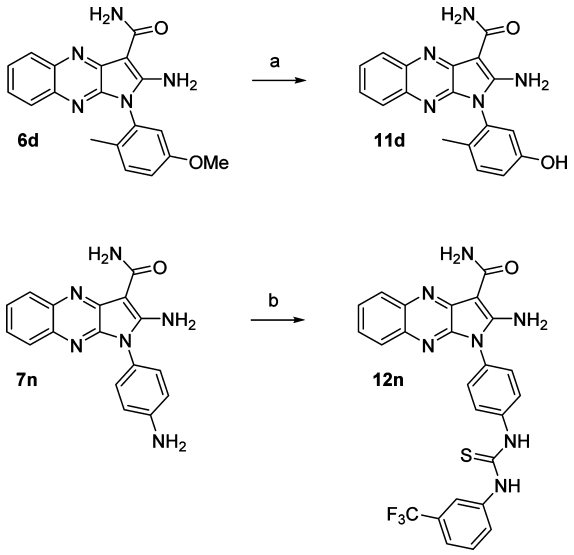

[a]Reagents and conditions: (a) BBr_3, DCM, 130 °C, 4 h, 68%; (b) *m*-CF_3-phenyl isothiocyanate, DMF, 25 °C, 12 h, 69%.

substituted quinoxalines, which is in agreement with previously reported kinase inhibitors[20,42−47] and could be a consequence of restricting the accessible conformations of the phenyl ring as we have previously reported.[20] However, the *ortho*-fluoro substituted inhibitor **6g** or bis-*ortho* substituted **6b** and **6c** caused a lower stabilization of the protein probably due to the small size of fluorine or the introduction of an extra steric bulk, respectively.

The transition from type I to type $I_{1/2}$ by the presence of a hydrogen bond donor at position R_3, and therefore the formation of hydrogen bonds with Glu664 and Asp758, resulted in a remarkable increase in thermal shift for compound **6h** (7.2 °C), which became more pronounced upon introduction of a methyl group in the ortho-relative position (following the trend observed in type I inhibitors) to yield **11d** with a thermal shift of 11.2 °C.

Type II compounds bearing an amide linker followed by a *m*-CF_3-phenyl group caused a similar stabilization effect in the protein as the type $I_{1/2}$ inhibitor **11d**. As expected from previous results with type I and $I_{1/2}$ compounds, the addition of a methyl (**7c** and **7h**) or fluorine (**7d** and **7i**) substituent in R_1 lead to higher thermal shifts. Interestingly, 3-amides (**7g−i**) triggered a higher stabilization of the kinase than 1-amides (**7b−d**), which could indicate the formation of a more favorable hydrogen bond with Glu664. The presence of imidazoles within the allosteric binding site led to compounds **7e** and **7j**, which showed the most promising thermal shifts (16 °C). Urea (**7m**) or thiourea (**12n**) linkers located in para-relative position retained or even enhanced (in the case of urea **7m**) the binding affinity, whereas compound **7l**, bearing the urea in meta-relative position barely presented any thermal shift, suggesting a disruption or a nonfavorable hydrogen bond interaction with Glu664. The replacement of the *m*-CF_3-phenyl group by a cyclopropyl ring proved to be detrimental in all cases, and no thermal shift was observed for products **7a**, **7f**, and **7k**.

The inhibitory activities of type I and type $I_{1/2}$ inhibitors were further evaluated on an enzymatic assay based on fluorescence resonance transfer (FRET) at a single concentration (1 μM, Table 1, column 8). The results were in line with the thermal shifts described above. Compounds **6a** and **6f** showed inhibitory activities higher than 66% at 1 μM (Table 1). However, substitution at R_1 by a smaller fluorine atom yielded compound **6g** with lower binding affinity (30%). Along the same lines, bis-*ortho* substitutions with either methyl or chlorine (**6b**,**c**) decreased the binding affinity (36 and 45% inhibitory activities, respectively) probably due to unfavorable steric effects. The presence of a hydrogen bond donor at R_3 (type $I_{1/2}$ inhibitors) either as a phenol (**6h** and **11d**) or methylene alcohol (**6e**) greatly improved the inhibitory activity of the molecules thanks to the formation of hydrogen bonds with Glu664 and Asp758 (68−105%). To our surprise, a triazole group at the same position (**6i**) dramatically decreased the binding affinity (7%).

The kinetics of binding of the optimized type $I_{1/2}$ (**11d**) and type II urea inhibitor (**7m**) were investigated using SPR. Upon titrating **11d** and **7m** over immobilized dephosphorylated EphA3, dissociation constants (K_D) in the low nanomolar range were obtained (8.6 and 39.3 nM, respectively), confirming the high affinity of the compounds (Figure 2). One of the

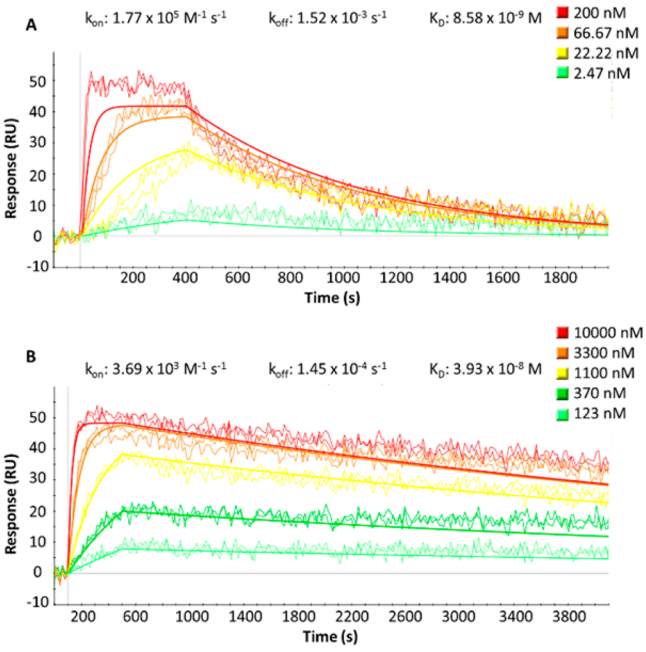

Figure 2. SPR analysis of the binding of **11d** (A) and **7m** (B) to EphA3. A 3-fold serial dilution of the compounds was made starting from 200 nM (for **11d**) and 10 μM (for **7m**) in duplicate. The theoretical global fit to a 1:1 interaction model is shown in straight lines.

advantageous characteristics of type II inhibitors over type I or $I_{1/2}$ is their slow dissociation rate from the target protein,[48−50] as demonstrated by the remarkably slow k_{off} measured for **7m** (1.45×10^{-4} s^{-1}) in comparison to the type $I_{1/2}$ **11d** (1.52×10^{-3} s^{-1}). The slow k_{off} of **7m** corresponds to a residence time of 115 min, a value that compares positively with that of marketed drugs such as imatinib (28 min for dephosphorylated ABL), nilotinib (202 and 205 min for dephosphorylated and phosphorylated ABL, respectively), and dasatinib (15 and 4 min).[51] The long residence time of type II inhibitors is considered to be beneficial for drug efficacy and selectivity *in vivo* due to the high concentration of the drug near the

target,[50,52] as described for the EGFR-specific inhibitor lapatinib.[53]

IV. VALIDATION OF TYPE II BINDING BY X-RAY CRYSTAL STRUCTURE DETERMINATION

The crystal structure of the catalytic domain of the EphA3 kinase in complex with inhibitor **7m** (solved at 2.0 Å resolution, Supporting Information S34) confirms a type II binding mode, i.e., with the DFG-out conformation (Figure 3). The pyrrolo[3,2-*b*]quinoxaline scaffold occupies the ATP binding site and is involved in the same hydrogen bonds with the hinge region as the type I inhibitor **A** (Figure 1). In addition, the urea linker of inhibitor **7m** acts as hydrogen bond acceptor from the Ser757 side chain and the amide backbone of Asp758, and hydrogen bond donor to the side chain of Glu664. The *m*-CF_3-phenyl moiety is nestled in the hydrophobic pocket, which originates from the displacement of the Phe side chain of the DFG motif. Thus, the type II binding mode of compound **7m** validates our design based on the crystal structures of the complexes with the type I inhibitors (*vide supra*, section II.2).

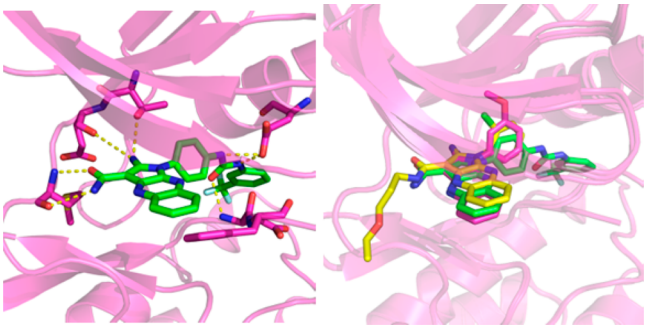

Figure 3. Crystal structures of the catalytic domain of the tyrosine kinase EphA3 in complex with the low-nanomolar inhibitor **7m** (left, pdb code 4P5Z) and superposition of the three inhibitors **A**, **B**, and **7m** based on structural alignment of the C_α atoms of the EphA3 kinase domain (right). The ATP binding site of the EphA3 kinase is shown in magenta ribbons, while the side chains mentioned in the text and the inhibitors are shown by sticks.

V. SELECTIVITY AND CELLULAR ACTIVITY

V.1. Selectivity Profiles from Biochemical Assays. The selectivity profile of inhibitors **11d**, **7b**, and **7g** was determined by an *in vitro* competition binding assay using recombinant kinases (KINOMEscan at DiscoveRx).[54] It is important to note that this assay reports on binding affinity and does not require ATP. The selectivity panel consisted of 453 human kinases, 58 of which were disease related mutant kinases (mainly of ABL1, EGFR, and PIK3CA). Single dose measurements were carried out at 1 μM concentration of the inhibitor.

Compounds **11d**, **7b**, and **7g** present a very similar selectivity profile (Figure 4); in particular, strong binding is only observed for tyrosine kinases with threonine as a gatekeeper residue, e.g., ABL1/2, BRAF, DDR1, EphA/B (all but EphA7, which has a Ile gatekeeper), KIT, LCK, SRC, and YES. The latter data suggest that most (or even all) tyrosine kinases with a Thr gatekeeper can assume the DFG-out conformation. Quantita-

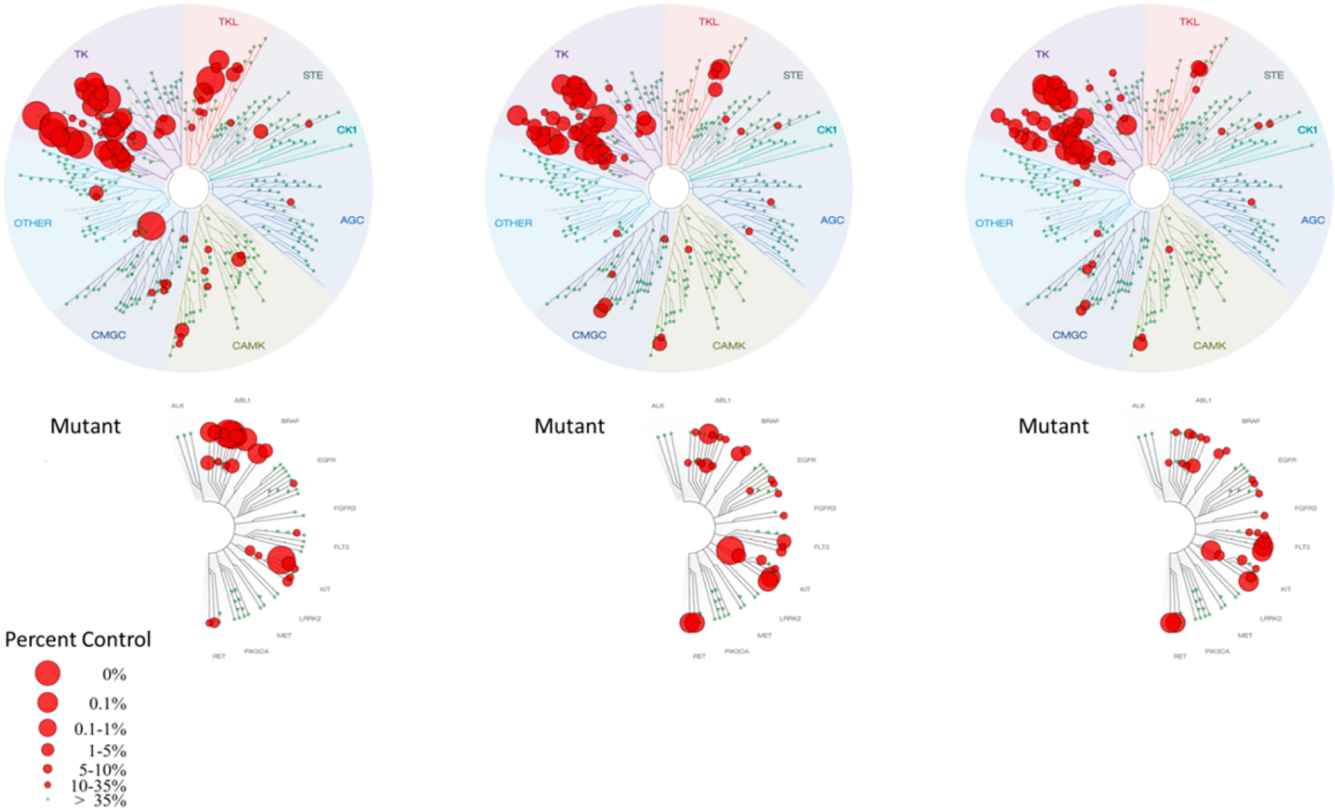

Figure 4. Selectivity profiles of compound **11d** (left), **7b** (center), and **7g** (right) tested on a panel of 395 nonmutant (top) and 58 mutant (bottom) kinases at DiscoveRx. Measurements were performed at a concentration of 1 μM of the inhibitor. The affinity is defined with respect to a DMSO control. The dendrogram was obtained from KinomeScan using the KinomeTree software.

tively, each of the three inhibitors **11d**, **7b**, and **7g** binds with an affinity 10-fold (100-fold) higher than the DMSO negative control to only about 10% (5%) of the 395 wild-type kinases tested. Interestingly, the selectivity profiles of the type $I_{1/2}$ (**11d**) and II (**7b** and **7g**) quinoxaline-based inhibitors is very similar to the one of our previously reported type I and $I_{1/2}$ xanthine-based inhibitors (compounds **40** and **3**, respectively, in ref 22), which is due, at least in part, to the use of an Eph tyrosine kinase (EphB4) as primary target for the *in silico* screening and optimization.

V.2. Cellular Assays. The most potent inhibitors obtained in the optimization campaign were further tested in cell-based assays. Cellular phosphorylation assays on MEF cells transfected with myc-tagged human EphB4 revealed a comparable tendency to the one observed in the enzymatic assay (Table 1, column 9). The type I inhibitors (**6a–d**) displayed cellular IC_{50} values in the 230–4400 nM range, with the *ortho*-methyl substituted derivative **6a** as the most potent member of this series. The type $I_{1/2}$ inhibitor **11d** and type II compounds bearing amide linkers and a *m*-CF_3-phenyl group (**7b–d** and **7g–i**) displayed levels of inhibitory activity in the low nanomolar range (6–24 nM), thus being the most promising molecules of the optimization campaign. In agreement with thermal shift experiments, the presence of a urea (**7m**) and specially the thiourea linker (**12n**) decreased the potency of the compounds (89 and 560 nM, respectively). Interestingly, the imidazole substituted compounds (**7e** and **7j**) proved to be the weakest type II inhibitors (170 and 270 nM, respectively) in contrast to the high thermal shifts obtained (16 °C) in the differential scanning fluorimetry measurements, pointing toward potential cell permeability or efflux issues.

EphB4 overexpression has been linked to several types of cancer, including breast,[55] colon, [56] and ovarian.[57] Compounds **11d** and **7m** were screened against the NCI-60 cancer cell line panel (Supporting Information S3 and S4) displaying antiproliferative activities against leukemia (K-562), lung (HOP-92), colon (HT-29), renal (A498), and breast cancer cells (MDA-MB-231 and HS 578T) in the low nanomolar range. Driven by these results, the most promising inhibitors of our optimization campaign were tested in-house against the above-mentioned NCI cancer cell lines (Table 2). The leukemia K-562 cell line was particularly sensitive toward the optimized type II quinoxaline inhibitors, especially in the case of 3-amide compounds **7h** and **7i**, which showed remarkably low GI_{50} values (36 and 81 nM, respectively). Interestingly, similar levels of potency were found for imidazole substituted compounds **7e** and **7j**, which seemed to be among the weakest type II binders in the cellular phosphorylation assays, possibly indicating other targets than Eph for these molecules. In addition, the potential of **11d** (the most potent compound on cellular phosphorylation assays with an IC_{50} of 6 nM) to inhibit the growth of patient-derived tumor cell lines was studied using a propidium iodide-based proliferation assay and dasatinib as a reference (Oncotest, Table 3). Cell lines included colon, lung, kidney, pancreatic, prostate, and stomach cancer cells. Whereas dasatinib presented double-digit nanomolar activities against RXF 393NL, LXFA 983L, and PRXF DU145, **11d** exhibited low micromolar GI_{50} values, with RXF 393NL being the most sensitive cell line.

The implication of EphB4-ephrinB2 signaling in sprouting angiogenesis and blood vessel maturation[58] and the inhibition of vascular endothelial growth factor (VEGFR)-driven angiogenesis by the selective EphB4 inhibitor NVP-BHG712,[59] led us to examine the efficacy of **11d** on human endothelial cell sprouting in a spheroid based cellular angiogenesis assay (ProQinase, Supporting Information S36).[60] Compound **11d** was able to successfully inhibit VEGF-A induced HUVEC (primary human umbilical vein endothelial cells) sprouting in a dose dependent manner with an IC_{50} value of 1.5 μM.

Table 2. Antiproliferative Activity against NCI Tumor Cell Lines[a]

compd	MDA -MB-231	K-562	A498	HT29	KM12	HOP-92
6d			59.3	50.3		
6e		44.9	36.4	90.5		
6i			50.9	64.5		
11d	2.64	1.05	5.88	4.59	1.55	0.49
7b	3.09	1.52	13.4	29.4	3.98 (4.03)	4.65 (3.91)
7c	3.88	0.73	2.50	5.87	0.80	4.23
7d	1.44	0.37	1.88	1.80 (9.43)	2.16	2.06
7e	1.93	0.030	4.01	13.4	2.54	5.12
7g	10.8	0.820	10.6	23.1	2.78	5.13
7h	1.32	0.036	2.07	2.82	1.57	1.92
7i	2.69	0.081	2.44	2.97	1.87	2.12
7j	3.05	0.029	5.71	4.36	2.84	3.01
7m	10.3	5.45	10.8	18.0	0.67	10.0
12n	9.63	5.07	8.73	16.3	2.52	14.25

[a] GI_{50} values were determined using resazurin reduction after 2–3 days of incubation with the corresponding compound. GI_{50} values are given in micromolar concentrations (μM) as the mean of at least three independent experiments. Variability around the mean value was <50% unless otherwise indicated by an SE value in parentheses.

Table 3. Antiproliferative Activity against Patient Derived Tumor Cell Lines[a]

compd	**11d**	dasatinib
RXF 393NL	0.725	0.0217
CXF 1103L	3.83	4.36
LXFA 983L	2.22	0.0565
GXF 251L	8.01	2.25
PAXF 1657L	2.92	0.121
PRXF DU145	2.92	0.0623

[a] GI_{50} values were determined at Oncotest using a modified propidium iodide assay. Measurements were performed after 4 days of incubation with **11d** and dasatinib. GI_{50} values are given in micromolar concentrations (μM).

VI. *IN VIVO* DATA

Three of the most promising compounds from these series (**7b**, **7g**, and **11d**) were selected for evaluation of pharmacokinetic properties in 20–30 g male CD-1 (ICR) mice on intravenous (IV) and oral (PO) administration. Low to moderate oral bioavailability of tested compounds in mice was observed, with compounds **11d** and **7g** giving the highest values (Table 4). Promising cellular efficacy and pharmacokinetic properties incited the subsequent evaluation of compound **11d** in a xenograft mouse model with a tumor derived from the MDA-MB-231 cell line. High compound clearance (Cl) and moderate half-life ($t_{1/2}$) values determined in the pharmacokinetic study motivated a twice-daily dosing regime totaling 100 mg/kg/day of compound **11d** over 21 days. Median tumor volume

Table 4. Pharmacokinetic Properties in Mice

compd	11d		7b		7g	
	iv	po	iv	po	iv	po
dose (mg/kg)	1	5	1	5	1	5
Cl (mL/min/kg)	42		32		31	
V_{ss} (L/kg)	1.6		2.2		2.2	
$t_{1/2}$ (h)	1.7	1.7	1.2	5.0	1.1	2.8
AUC_{last} (h·ng/mL)	392	493	506	263	533	803
F (%)		25		10		30

progression over time, starting from 108 mm^3, of both treatment and control cohorts is given in Figure 5.

In this study, median treatment-group tumor volume remained essentially stable throughout the treatment period, achieving a median tumor volume of 126 mm^3 at day 19 as opposed to the control group whose median tumor reached 650 mm^3 in the same period. Tumor growth inhibition (%TGI) was statistically significant (Mann−Whitney $U = 0$, $P \leq 0.001$, two-tailed) and quantified at 81% relative to the control group. Mean body weight of the treatment cohort decreased up to 16.3% of the initial mean body weight of this cohort during the treatment period. Treatment with compound **11d** provides a significant limitation in tumor progression over the control, suggesting that further studies of such xenograft model at lower doses of compound **11d** might provide tumor volume control with lessened weight loss. The further evaluation of compounds **11d** on mouse models of K-562 leukemia is underway.

VII. CONCLUSIONS

The X-ray crystal structures of the EphA3 kinase in complex with two high-nanomolar inhibitors based on the 2-amino-1-phenyl-pyrrolo[3,2-*b*]quinoxaline-3-carboxamide scaffold confirmed the type I binding mode obtained previously by automatic docking (Figure 1). This structural information was used to design type $I_{1/2}$ and type II derivatives by taking advantage of the existing knowledge on privileged chemical motifs, i.e., hydroxyl group in meta position of the phenyl ring (for type $I_{1/2}$) and hydrophobic moieties connected to the phenyl ring by amide or urea linkers (on type II). Chemical synthesis of ca. 25 derivatives (Table 1) culminated in several low nanomolar inhibitors with a good selectivity profile (Figure 4). The X-ray crystal structure of the EphA3 kinase in the complex with the inhibitor **7m** (Figure 3) provided the final validation of the structure-based design; in particular, the DFG-out conformation confirmed the type II binding. Moreover, the slow kinetics of unbinding of compound **7m** (measured by SPR, Figure 2) is congruent with the type II binding mode. Three interesting observations emerge from this study. First, it is possible to "elongate" a type $I_{1/2}$ into a type II inhibitor by introducing an amide or urea linked to a bulky hydrophobic group. These type II linkers are involved in the same hydrogen bonds as the type $I_{1/2}$ bearing a hydroxyl group in the same position, while the hydrophobic moiety occupies the pocket resulting from the displacement of the Phe side chain of the DFG motif. The similar selectivity profiles of type $I_{1/2}$ and type II inhibitors indicate that mainly the moiety in contact with the gatekeeper's side chain and hinge region determines specificity. Finally, *in vivo* assays (mice xenografted with human breast cancer) confirmed the cytostatic activity of one of our inhibitors (**11d**), which makes this type $I_{1/2}$ compound a candidate lead for further preclinical development.

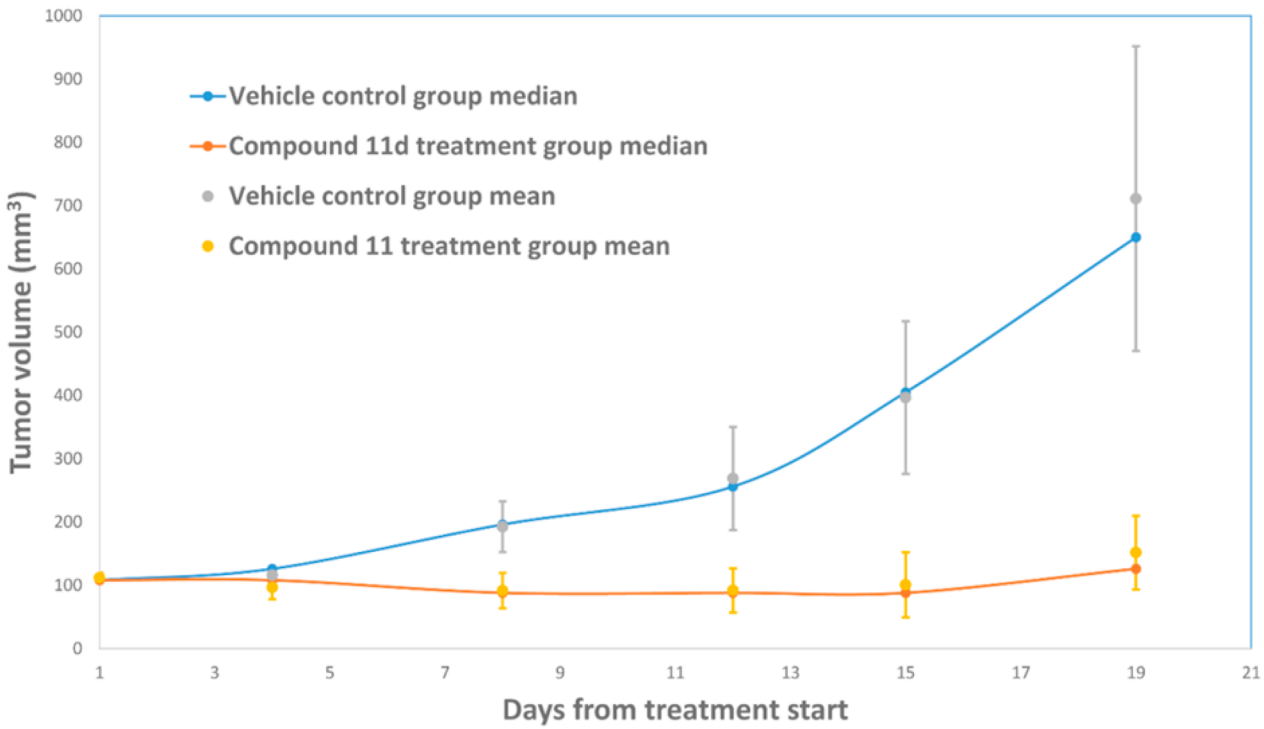

Figure 5. *In vivo* antitumor activity of compound **11d** in MDA-MB-231 nude mice xenografts. The mice received by gavage twice-daily 50 mg/kg of compound **11d** (red) or vehicle control (blue). Each data point is the median or mean of a cohort of 9 animals. Error bars show standard deviations of the mean.

■ ASSOCIATED CONTENT

Supporting Information

General procedures for the synthesis and characterization, biological evaluation of all reported compounds, and X-ray crystal structure refinement data. This material is available free of charge via the Internet at http://pubs.acs.org.

Accession Codes

PDB codes for EphA3 in complex with the inhibitors **A**, **B**, and **7m** are 4P4C, 4P5Q, and 4P5Z, respectively.

■ AUTHOR INFORMATION

Corresponding Authors

*(C.N.) E-mail: cristina.nevado@chem.uzh.ch. Phone: (41) 446353945. Fax: (41) 446353948.

*(A.C.) E-mail: caflisch@bioc.uzh.ch.

Author Contributions

[§]A.U. and J.D. contributed equally to this work.

Notes

The authors declare no competing financial interest.

■ ACKNOWLEDGMENTS

We thank Dr. Danzhi Huang for interesting discussions. We also thank Prof. Sirano Dhe-Paganon for providing the plasmid used for EphA3 expression. The authors would like to thank the Swiss National Science Foundation and the Swiss Cancer League (Krebsliga) for financial support.

■ ABBREVIATIONS USED

Eph, erythropoietin-producing human hepatocellular carcinoma receptor; DFG, aspartate-phenylalanine-glycine; ATP, adenosine triphosphate; SPR, surface plasmon resonance; DMF, dimethylformamide; TBTU, *N*,*N*,*N*′,*N*′-tetramethyl-*O*-(benzotriazol-1-yl)uronium tetrafluoroborate; DIPEA, diisoproylethylamine; DCM, dichloromethane; THF, tetrahydrofuran; HOBt, hydroxybenzotriazole; EDC, *N*-(3-(dimethylamino)propyl)-*N*′-ethylcarbodiimide; FRET, fluorescence-resonance energy transfer; Abl, abelson murine leukemia viral oncogene homologue; EGFR, epidermal growth factor receptor; DDR, discoidin domain receptor; Lck, lymphocyte-specific kinase; DMSO, dimethyl sulfoxide; MEF, mouse embryonic fibroblasts; VEGF, vascular endothelial growth factor; HUVEC, human umbilical vein endothelial cells

■ REFERENCES

(1) Manning, G.; Whyte, D. B.; Martinez, R.; Hunter, T.; Sudarsanam, S. The protein kinase complement of the human genome. *Science* **2002**, *298*, 1912−1934.

(2) Cohen, P. Protein kinases: the major drug targets of the twenty-first century? *Nat. Rev. Drug Discovery* **2002**, *1*, 309−315.

(3) Li, R.; Stafford, J. A. *Kinase Inhibitor Drugs*; John Wiley & Sons, Inc.: Hoboken, NJ, 2009.

(4) Blanc, J.; Geney, R.; Menet, C. Type II kinase inhibitors: an opportunity in cancer for rational design. *Anticancer Agents Med. Chem.* **2013**, *13*, 731−747.

(5) Kontzias, A.; Kotlyar, A.; Laurence, A.; Changelian, P.; O'Shea, J. J. Jakinibs: a new class of kinase inhibitors in cancer and autoimmune disease. *Curr. Opin. Pharmacol.* **2012**, *12*, 464−470.

(6) O'Brien, Z.; Moghaddam, M. F. Small molecule kinase inhibitors approved by the FDA from 2000 to 2011: a systematic review of preclinical ADME data. *Expert Opin. Drug Metab. Toxicol.* **2013**, *9*, 1597−1612.

(7) Zhang, J.; Yang, P. L.; Gray, N. S. Targeting cancer with small molecule kinase inhibitors. *Nat. Rev. Cancer* **2009**, *9*, 28−39.

(8) Janne, P. A.; Gray, N.; Settleman, J. Factors underlying sensitivity of cancers to small-molecule kinase inhibitors. *Nat. Rev. Drug Discovery* **2009**, *8*, 709−723.

(9) Liu, Q. S.; Sabnis, Y.; Zhao, Z.; Zhang, T. H.; Buhrlage, S. J.; Jones, L. H.; Gray, N. S. Developing irreversible inhibitors of the protein kinase cysteinome. *Chem. Biol.* **2013**, *20*, 146−159.

(10) Garuti, L.; Roberti, M.; Bottegoni, G. Irreversible protein kinase inhibitors. *Curr. Med. Chem.* **2011**, *18*, 2981−2994.

(11) Cozza, G.; Bortolato, A.; Menta, E.; Cavalletti, E.; Spinelli, S.; Moro, S. ATP non-competitive Ser/Thr kinase inhibitors as potential anticancer agents. *Anticancer Agents Med. Chem.* **2009**, *9*, 778−786.

(12) Liu, Y.; Gray, N. S. Rational design of inhibitors that bind to inactive kinase conformations. *Nat. Chem. Biol.* **2006**, *2*, 358−364.

(13) Traxler, P.; Furet, P. Strategies toward the design of novel and selective protein tyrosine kinase inhibitors. *Pharmacol. Ther.* **1999**, *82*, 195−206.

(14) Huang, D.; Zhou, T.; Lafleur, K.; Nevado, C.; Caflisch, A. Kinase selectivity potential for inhibitors targeting the ATP binding site: a network analysis. *Bioinformatics* **2010**, *26*, 198−204.

(15) Bamborough, P.; Drewry, D.; Harper, G.; Smith, G. K.; Schneider, K. Assessment of chemical coverage of kinome space and its implications for kinase drug discovery. *J. Med. Chem.* **2008**, *51*, 7898−7914.

(16) Karaman, M. W.; Herrgard, S.; Treiber, D. K.; Gallant, P.; Atteridge, C. E.; Campbell, B. T.; Chan, K. W.; Ciceri, P.; Davis, M. I.; Edeen, P. T.; Faraoni, R.; Floyd, M.; Hunt, J. P.; Lockhart, D. J.; Milanov, Z. V.; Morrison, M. J.; Pallares, G.; Patel, H. K.; Pritchard, S.; Wodicka, L. M.; Zarrinkar, P. P. A quantitative analysis of kinase inhibitor selectivity. *Nat. Biotechnol.* **2008**, *26*, 127−132.

(17) Morphy, R. Selectively nonselective kinase inhibition: striking the right balance. *J. Med. Chem.* **2010**, *53*, 1413−1437.

(18) Davis, M. I.; Hunt, J. P.; Herrgard, S.; Ciceri, P.; Wodicka, L. M.; Pallares, G.; Hocker, M.; Treiber, D. K.; Zarrinkar, P. P. Comprehensive analysis of kinase inhibitor selectivity. *Nat. Biotechnol.* **2011**, *29*, 1046−1051.

(19) Eglen, R.; Reisine, T. Drug discovery and the human kinome: recent trends. *Pharmacol. Ther.* **2011**, *130*, 144−156.

(20) Lafleur, K.; Huang, D.; Zhou, T.; Caflisch, A.; Nevado, C. Structure-based optimization of potent and selective inhibitors of the tyrosine kinase erythropoietin producing human hepatocellular carcinoma receptor B4 (EphB4). *J. Med. Chem.* **2009**, *52*, 6433−6446.

(21) Zhao, H. T.; Dong, J.; Lafleur, K.; Nevado, C.; Caflisch, A. Discovery of a novel chemotype of tyrosine kinase inhibitors by fragment-based docking and molecular dynamics. *ACS Med. Chem. Lett.* **2012**, *3*, 834−838.

(22) Lafleur, K.; Dong, J.; Huang, D.; Caflisch, A.; Nevado, C. Optimization of inhibitors of the tyrosine kinase EphB4. 2. Cellular potency improvement and binding mode validation by X-ray crystallography. *J. Med. Chem.* **2013**, *56*, 84−96.

(23) Boyd, A. W.; Bartlett, P. F.; Lackmann, M. Therapeutic targeting of EPH receptors and their ligands. *Nat. Rev. Drug Discovery* **2014**, *13*, 39−62.

(24) Zhao, H.; Huang, D. Hydrogen bonding penalty upon ligand binding. *PLoS One* **2011**, *6*, e19923.

(25) Zuccotto, F.; Ardini, E.; Casale, E.; Angiolini, M. Through the "gatekeeper door": exploiting the active kinase conformation. *J. Med. Chem.* **2010**, *53*, 2681−2694.

(26) Bold, G.; Altmann, K. H.; Frei, J.; Lang, M.; Manley, P. W.; Traxler, P.; Wietfeld, B.; Bruggen, J.; Buchdunger, E.; Cozens, R.; Ferrari, S.; Furet, P.; Hofmann, F.; Martiny-Baron, G.; Mestan, J.; Rosel, J.; Sills, M.; Stover, D.; Acemoglu, F.; Boss, E.; Emmenegger, R.; Lasser, L.; Masso, E.; Roth, R.; Schlachter, C.; Vetterli, W. New anilinophthalazines as potent and orally well absorbed inhibitors of the VEGF receptor tyrosine kinases useful as antagonists of tumor-driven angiogenesis. *J. Med. Chem.* **2000**, *43*, 2310−2323.

(27) Smith, R. A.; Barbosa, J.; Blum, C. L.; Bobko, M. A.; Caringal, Y. V.; Dally, R.; Johnson, J. S.; Katz, M. E.; Kennure, N.; Kingery-Wood, J.; Lee, W.; Lowinger, T. B.; Lyons, J.; Marsh, V.; Rogers, D. H.; Swartz, S.; Walling, T.; Wild, H. Discovery of heterocyclic ureas as a

new class of raf kinase inhibitors: identification of a second generation lead by a combinatorial chemistry approach. *Bioorg. Med. Chem. Lett.* **2001**, *11*, 2775−2778.

(28) Khire, U. R.; Bankston, D.; Barbosa, J.; Brittelli, D. R.; Caringal, Y.; Carlson, R.; Dumas, J.; Gane, T.; Heald, S. L.; Hibner, B.; Johnson, J. S.; Katz, M. E.; Kennure, N.; Kingery-Wood, J.; Lee, W.; Liu, X. G.; Lowinger, T. B.; McAlexander, I.; Monahan, M. K.; Natero, R.; Renick, J.; Riedl, B.; Rong, H.; Sibley, R. N.; Smith, R. A.; Wolanin, D. Omega-carboxypyridyl substituted ureas as Raf kinase inhibitors: SAR of the amide substituent. *Bioorg. Med. Chem. Lett.* **2004**, *14*, 783−786.

(29) Albaugh, P.; Fan, Y.; Mi, Y.; Sun, F. X.; Adrian, F.; Li, N. X.; Jia, Y.; Sarkisova, Y.; Kreusch, A.; Hood, T.; Lu, M.; Liu, G. X.; Huang, S. L.; Liu, Z. S.; Loren, J.; Tuntland, T.; Karanewsky, D. S.; Seidel, H. M.; Molteni, V. Discovery of GNF-5837, a selective TRK inhibitor with efficacy in rodent cancer tumor models. *ACS Med. Chem. Lett.* **2012**, *3*, 140−145.

(30) Liu, C.; Lin, J.; Wrobleski, S. T.; Lin, S.; Hynes, J.; Wu, H.; Dyckman, A. J.; Li, T.; Wityak, J.; Gillooly, K. M.; Pitt, S.; Shen, D. R.; Zhang, R. F.; McIntyre, K. W.; Salter-Cid, L.; Shuster, D. J.; Zhang, H.; Marathe, P. H.; Doweyko, A. M.; Sack, J. S.; Kiefer, S. E.; Kish, K. F.; Newitt, J. A.; McKinnon, M.; Dodd, J. H.; Barrish, J. C.; Schieven, G. L.; Leftheris, K. Discovery of 4-(5-(cyclopropylcarbamoyl)-2-methylphenylamino)-5-methyl-*N*-propylpyrrolo[1,2-f][1,2,4]triazine-6-carboxamide (BMS-582949), a clinical p38α MAP kinase inhibitor for the treatment of inflammatory diseases. *J. Med. Chem.* **2010**, *53*, 6629−6639.

(31) Hynes, J., Jr.; Wu, H.; Pitt, S.; Shen, D. R.; Zhang, R.; Schieven, G. L.; Gillooly, K. M.; Shuster, D. J.; Taylor, T. L.; Yang, X.; McIntyre, K. W.; McKinnon, M.; Zhang, H.; Marathe, P. H.; Doweyko, A. M.; Kish, K.; Kiefer, S. E.; Sack, J. S.; Newitt, J. A.; Barrish, J. C.; Dodd, J.; Leftheris, K. The discovery of (*R*)-2-(sec-butylamino)-*N*-(2-methyl-5-(methylcarbamoyl)phenyl) thiazole-5-carboxamide (BMS-640994): A potent and efficacious p38α MAP kinase inhibitor. *Bioorg. Med. Chem. Lett.* **2008**, *18*, 1762−1767.

(32) Wrobleski, S. T.; Lin, S.; Dhar, T. G.; Dyckman, A. J.; Li, T.; Pitt, S.; Zhang, R.; Fan, Y.; Doweyko, A. M.; Tokarski, J. S.; Kish, K. F.; Kiefer, S. E.; Sack, J. S.; Newitt, J. A.; Witmer, M. R.; McKinnon, M.; Barrish, J. C.; Dodd, J. H.; Schieven, G. L.; Leftheris, K. The identification of novel p38α isoform selective kinase inhibitors having an unprecedented p38α binding mode. *Bioorg. Med. Chem. Lett.* **2013**, *23*, 4120−4126.

(33) Weisberg, E.; Manley, P. W.; Breitenstein, W.; Bruggen, J.; Cowan-Jacob, S. W.; Ray, A.; Huntly, B.; Fabbro, D.; Fendrich, G.; Hall-Meyers, E.; Kung, A. L.; Mestan, J.; Daley, G. Q.; Callahan, L.; Catley, L.; Cavazza, C.; Azam, M.; Neuberg, D.; Wright, R. D.; Gilliland, D. G.; Griffin, J. D. Characterization of AMN107, a selective inhibitor of native and mutant Bcr-Abl. *Cancer Cell* **2005**, *7*, 129−141.

(34) Ishikawa, M.; Hashimoto, Y. Improvement in aqueous solubility in small molecule drug discovery programs by disruption of molecular planarity and symmetry. *J. Med. Chem.* **2011**, *54*, 1539−1554.

(35) Pratt, E. F.; Kereszte, J. Syntheses of indolizino- and dihydroindolizinoquinoxalines. *J. Org. Chem.* **1967**, *32*, 49−53.

(36) Obafemi, C. A.; Pfleiderer, W. Synthesis and some reactions of 3-chloro-2-(cyanomethylene)-1,2-dihydroquinoxalines. *Molecules* **2004**, *9*, 223−231.

(37) Otomasu, H.; Ohmiya, S.; Sekuguch, T.; Takahash, H. Synthesis of condensed quinoxalines 0.2. A new synthesis of pyrrolo- 2,3-b-quinoxalines. *Chem. Pharm. Bull.* **1970**, *18*, 2065.

(38) Choi, H. G.; Ren, P.; Adrian, F.; Sun, F.; Lee, H. S.; Wang, X.; Ding, Q.; Zhang, G.; Xie, Y.; Zhang, J.; Liu, Y.; Tuntland, T.; Warmuth, M.; Manley, P. W.; Mestan, J.; Gray, N. S.; Sim, T. A type-II kinase inhibitor capable of inhibiting the T315I "gatekeeper" mutant of Bcr-Abl. *J. Med. Chem.* **2010**, *53*, 5439−5448.

(39) Huang, W. S.; Shakespeare, W. C. An efficient synthesis of nilotinib (AMN107). *Synthesis-Stuttgart* **2007**, 2121−2124.

(40) Jung, M. E.; Ouk, S.; Yoo, D.; Sawyers, C. L.; Chen, C.; Tran, C.; Wongvipat, J. Structure−activity relationship for thiohydantoin androgen receptor antagonists for castration-resistant prostate cancer (CRPC). *J. Med. Chem.* **2010**, *53*, 2779−2796.

(41) Niesen, F. H.; Berglund, H.; Vedadi, M. The use of differential scanning fluorimetry to detect ligand interactions that promote protein stability. *Nat. Protoc.* **2007**, *2*, 2212−2221.

(42) Wang, Y.; Shakespeare, W. C.; Huang, W. S.; Sundaramoorthi, R.; Lentini, S.; Das, S.; Liu, S.; Banda, G.; Wen, D.; Zhu, X.; Xu, Q.; Keats, J.; Wang, F.; Wardwell, S.; Ning, Y.; Snodgrass, J. T.; Broudy, M. I.; Russian, K.; Dalgarno, D.; Clackson, T.; Sawyer, T. K. Novel N9-arenethenyl purines as potent dual Src/Abl tyrosine kinase inhibitors. *Bioorg. Med. Chem. Lett.* **2008**, *18*, 4907−4912.

(43) Bamborough, P.; Angell, R. M.; Bhamra, I.; Brown, D.; Bull, J.; Christopher, J. A.; Cooper, A. W.; Fazal, L. H.; Giordano, I.; Hind, L.; Patel, V. K.; Ranshaw, L. E.; Sims, M. J.; Skone, P. A.; Smith, K. J.; Vickerstaff, E.; Washington, M. *N*-4-Pyrimidinyl-1*H*-indazol-4-amine inhibitors of Lck: indazoles as phenol isosteres with improved pharmacokinetics. *Bioorg. Med. Chem. Lett.* **2007**, *17*, 4363−4368.

(44) Angell, R. M.; Angell, T. D.; Bamborough, P.; Brown, D.; Brown, M.; Buckton, J. B.; Cockerill, S. G.; Edwards, C. D.; Jones, K. L.; Longstaff, T.; Smee, P. A.; Smith, K. J.; Somers, D. O.; Walker, A. L.; Willson, M. Biphenyl amide p38 kinase inhibitors 2: Optimisation and SAR. *Bioorg. Med. Chem. Lett.* **2008**, *18*, 324−328.

(45) Graham Robinett, R.; Freemerman, A. J.; Skinner, M. A.; Shewchuk, L.; Lackey, K. The discovery of substituted 4-(3-hydroxyanilino)-quinolines as potent RET kinase inhibitors. *Bioorg. Med. Chem. Lett.* **2007**, *17*, 5886−5893.

(46) Hynes, J., Jr.; Dyckman, A. J.; Lin, S.; Wrobleski, S. T.; Wu, H.; Gillooly, K. M.; Kanner, S. B.; Lonial, H.; Loo, D.; McIntyre, K. W.; Pitt, S.; Shen, D. R.; Shuster, D. J.; Yang, X.; Zhang, R.; Behnia, K.; Zhang, H.; Marathe, P. H.; Doweyko, A. M.; Tokarski, J. S.; Sack, J. S.; Pokross, M.; Kiefer, S. E.; Newitt, J. A.; Barrish, J. C.; Dodd, J.; Schieven, G. L.; Leftheris, K. Design, synthesis, and anti-inflammatory properties of orally active 4-(phenylamino)-pyrrolo[2,1-f][1,2,4]-triazine p38α mitogen-activated protein kinase inhibitors. *J. Med. Chem.* **2008**, *51*, 4−16.

(47) Deak, H. L.; Newcomb, J. R.; Nunes, J. J.; Boucher, C.; Cheng, A. C.; DiMauro, E. F.; Epstein, L. F.; Gallant, P.; Hodous, B. L.; Huang, X.; Lee, J. H.; Patel, V. F.; Schneider, S.; Turci, S. M.; Zhu, X. *N*-(3-(Phenylcarbamoyl)arylpyrimidine)-5-carboxamides as potent and selective inhibitors of Lck: structure, synthesis and SAR. *Bioorg. Med. Chem. Lett.* **2008**, *18*, 1172−1176.

(48) Kufareva, I.; Abagyan, R. Type-II kinase inhibitor docking, screening, and profiling using modified structures of active kinase states. *J. Med. Chem.* **2008**, *51*, 7921−7932.

(49) Pargellis, C.; Tong, L.; Churchill, L.; Cirillo, P. F.; Gilmore, T.; Graham, A. G.; Grob, P. M.; Hickey, E. R.; Moss, N.; Pav, S.; Regan, J. Inhibition of p38 MAP kinase by utilizing a novel allosteric binding site. *Nat. Struct. Biol.* **2002**, *9*, 268−272.

(50) Copeland, R. A.; Pompliano, D. L.; Meek, T. D. Drug-target residence time and its implications for lead optimization. *Nat. Rev. Drug Discovery* **2006**, *5*, 730−739.

(51) Manley, P. W.; Cowan-Jacob, S. W.; Fendrich, G.; Jahnke, W.; Fabbro, D. Nilotinib, in Comparison to Both Dasatinib and Imatinib, Possesses a Greatly Prolonged Residence Time When Bound to the BCR-ABL Kinase SH1 Domain. 53rd ASH Annual Meeting and Exposition, San Diego, CA, 2011.

(52) Kitagawa, D.; Gouda, M.; Kirii, Y. Quick evaluation of kinase inhibitors by surface plasmon resonance using single-site specifically biotinylated kinases. *J. Biomol. Screening* **2014**, *19*, 453−461.

(53) Wood, E. R.; Truesdale, A. T.; McDonald, O. B.; Yuan, D.; Hassell, A.; Dickerson, S. H.; Ellis, B.; Pennisi, C.; Horne, E.; Lackey, K.; Alligood, K. J.; Rusnak, D. W.; Gilmer, T. M.; Shewchuk, L. A unique structure for epidermal growth factor receptor bound to GW572016 (Lapatinib): relationships among protein conformation, inhibitor off-rate, and receptor activity in tumor cells. *Cancer Res.* **2004**, *64*, 6652−6659.

(54) Fabian, M. A.; Biggs, W. H., III; Treiber, D. K.; Atteridge, C. E.; Azimioara, M. D.; Benedetti, M. G.; Carter, T. A.; Ciceri, P.; Edeen, P. T.; Floyd, M.; Ford, J. M.; Galvin, M.; Gerlach, J. L.; Grotzfeld, R. M.; Herrgard, S.; Insko, D. E.; Insko, M. A.; Lai, A. G.; Lelias, J. M.; Mehta, S. A.; Milanov, Z. V.; Velasco, A. M.; Wodicka, L. M.; Patel, H. K.;

Zarrinkar, P. P.; Lockhart, D. J. A small molecule-kinase interaction map for clinical kinase inhibitors. *Nat. Biotechnol.* **2005**, *23*, 329−336.
(55) Kumar, S. R.; Singh, J.; Xia, G.; Krasnoperov, V.; Hassanieh, L.; Ley, E. J.; Scehnet, J.; Kumar, N. G.; Hawes, D.; Press, M. F.; Weaver, F. A.; Gill, P. S. Receptor tyrosine kinase EphB4 is a survival factor in breast cancer. *Am. J. Pathol.* **2006**, *169*, 279−293.
(56) Stephenson, S. A.; Slomka, S.; Douglas, E. L.; Hewett, P. J.; Hardingham, J. E. Receptor protein tyrosine kinase EphB4 is up-regulated in colon cancer. *BMC Mol. Biol.* **2001**, *2*, 15.
(57) Castellano, G.; Reid, J. F.; Alberti, P.; Carcangiu, M. L.; Tomassetti, A.; Canevari, S. New potential ligand-receptor signaling loops in ovarian cancer identified in multiple gene expression studies. *Cancer Res.* **2006**, *66*, 10709−10719.
(58) Adams, R. H. Vascular patterning by Eph receptor tyrosine kinases and ephrins. *Semin. Cell Dev. Biol.* **2002**, *13*, 55−60.
(59) Martiny-Baron, G.; Holzer, P.; Billy, E.; Schnell, C.; Brueggen, J.; Ferretti, M.; Schmiedeberg, N.; Wood, J. M.; Furet, P.; Imbach, P. The small molecule specific EphB4 kinase inhibitor NVP-BHG712 inhibits VEGF driven angiogenesis. *Angiogenesis* **2010**, *13*, 259−267.
(60) Korff, T.; Augustin, H. G. Tensional forces in fibrillar extracellular matrices control directional capillary sprouting. *J. Cell Sci.* **1999**, *112* (Pt 19), 3249−3258.